1

An Adaptive Control for a Free-Floating Space Robot by Using Inverted Chain Approach

Satoko Abiko and Gerd Hirzinger
Institute of Robotics and Mechatronics, German Aerospace Center (DLR)
Germany

1. Introduction

On-orbit servicing space robots are one of the challenging fields in the robotics and space technology. The space robots are expected to perform various tasks including capturing a target, constructing a large structure and autonomous maintenance of on-orbit systems. In these space missions, one of the main tasks with the robotic system would be the tracking, the grasping and the positioning of a target in operational space. In this chapter, we address the task of following a desired trajectory in operational space while the space robot grasps a target with unknown dynamic properties. The dynamic uncertainty leads to a tracking problem, where a given nominal trajectory has to be tracked, while accounting for the parameter uncertainty.

In ground-based manipulator systems, the dynamic parameter uncertainty affects only dynamic equations. In free-floating space robots, however, the parameter uncertainty appears not only in the dynamic equations but also in kinematic mapping from the joint space to the Cartesian space due to the absence of a fixed base. Therefore, the model inaccuracies lead to the deviation of operational space trajectory provided by the kinematic mapping.

One method to deal with this issue can be found in an adaptive control. Xu and Gu proposed an adaptive control scheme for space robots in both joint space and operational space [Xu et al., 1992, Gu & Xu, 1993]. However, the adaptive control proposed in [Xu et al., 1992] requires perfect attitude control and the adaptive control in [Gu & Xu, 1993] is developed based on an under-actuated system on the assumption that the acceleration of the base-satellite is measurable.

In this chapter, we propose an adaptive control for a *fully* free-floating space robot in operational space. This chapter particularly focuses on the uncertainty of kinematic mapping, which includes the dynamic parameters of the system. To achieve the desired input torque, it is assumed here that the velocity-based closed-loop servo controller is used as noted in [Konno et al., 1997].

In the modeling of the space robot, we consider the system switched around since a free-floating space robot does not have any fixed base, and then the robotic system is modeled from the end-effector to the base-satellite. This approach was termed the *inverted chain approach* in [Abiko et al., 2006]. The inverted chain approach explicitly explains coupled dynamics between the end-effector and the robot arm. A proposed adaptive control for

operational space trajectory tracking is developed based on the inverted chain approach. The control method is verified in simulation for a realistic three-dimensional scenario (See Fig. 1).

The chapter is organized as follows. Section 2 describes the dynamic model of a space robot by the inverted chain approach. Section 3 discusses the operational space motion control for the space robot based on the passivity theorem. Section 4 proposes an adaptive control for trajectory tracking in operational space against parameter uncertainties. Section 5 derives an alternative adaptive control for performance improvement. Section 6 illustrates the simulation results with a three-dimensional realistic model. The conclusions are summarized in Section 7.

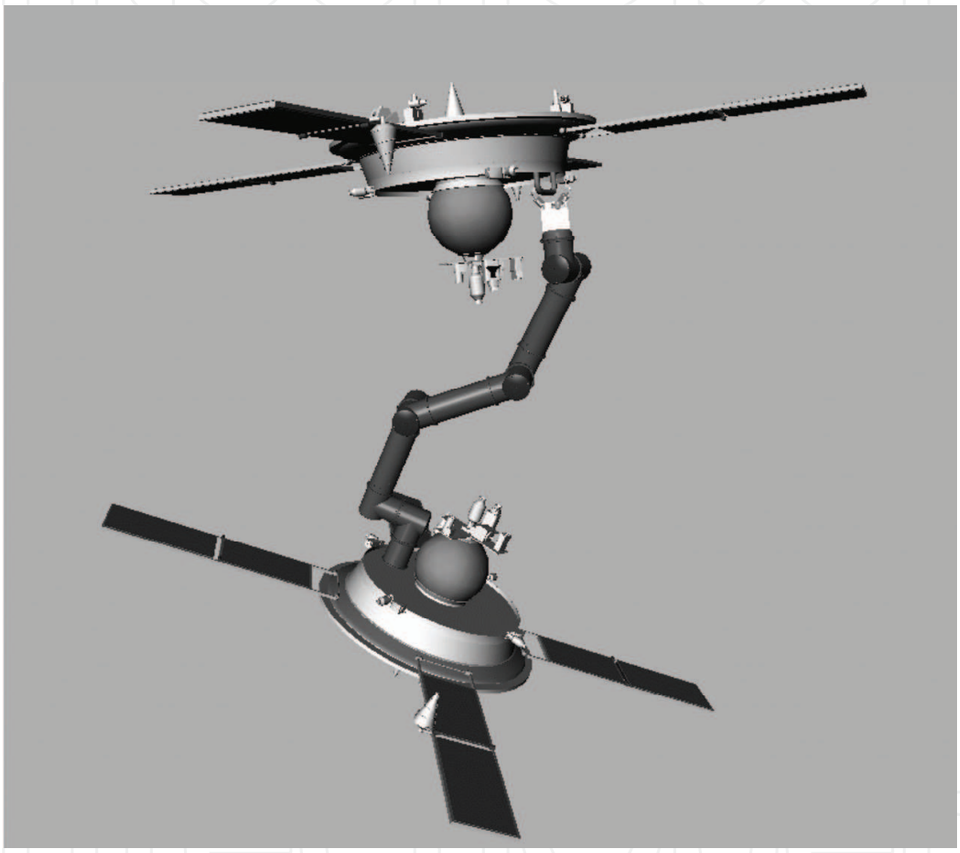

Figure 1. Chaser-robot and target scenario

2. Modeling and Equations of Motion

This section introduces the model of a space robot. Since the focus of this research is on following a desired trajectory in operational space, it is convenient to refer to operational space formulation.

Due to the lack of a fixed base, one can model a free-floating space robot with two approaches. The general dynamic expressions of the free-floating robot use linear and angular velocities of the base-satellite and the motion rate of each joint as the generalized coordinates [Xu & Kanade, 1993]. However, by considering the system switched around, modeled from the end-effector to the base, it can be represented by the motion of the end

effector and that of the joints in the same structure as in the conventional expression. This scheme is termed the *inverted chain approach.*
The following subsections explain the dynamic equations of the system in the inverted chain approach, for a serial rigid-link manipulator attached to a floating base, as shown in Fig. 2. The main notations used in this section are listed in Table 1.

2.1 Equations of motion - Inverted chain approach

Let us consider the linear and angular velocities of the end-effector, $\dot{\boldsymbol{x}}_e = (\boldsymbol{v}_e^T, \boldsymbol{\omega}_e^T)^T \in R^{6\times 1}$, and the motion rate of the joints, $\dot{\boldsymbol{\phi}} \in R^{n\times 1}$ as the generalized coordinates. The equations of motion are expressed in the following form:

$$\begin{bmatrix} \boldsymbol{H}_e & \boldsymbol{H}_{em} \\ \boldsymbol{H}_{em}^T & \boldsymbol{H}_m \end{bmatrix} \begin{bmatrix} \ddot{\boldsymbol{x}}_e \\ \ddot{\boldsymbol{\phi}} \end{bmatrix} + \begin{bmatrix} \boldsymbol{c}_e & \boldsymbol{c}_{em} \\ \boldsymbol{c}_{em}^T & \boldsymbol{c}_m \end{bmatrix} \begin{bmatrix} \dot{\boldsymbol{x}}_e \\ \dot{\boldsymbol{\phi}} \end{bmatrix} = \begin{bmatrix} \mathcal{F}_e \\ \boldsymbol{\tau} \end{bmatrix} + \begin{bmatrix} \boldsymbol{J}_e^T \\ \boldsymbol{J}_m^T \end{bmatrix} \mathcal{F}_b. \quad (1)$$

In the case that $\mathcal{F}_b$ is generated actively (*e.g.* jet thrusters or reaction wheels etc.), the system is called a *free-flying* robot. On the other hand, if no active actuators are applied on the base, the system is termed a *free-floating* robot. In this chapter, we consider the *free-floating* robot.
The dynamic equation (1) possesses following important properties.
Property 1: The inerta matrices $\boldsymbol{H}_e \in R^{6\times 6}$, $\boldsymbol{H}_m \in R^{n\times n}$ *and* $\boldsymbol{H} = \begin{bmatrix} \boldsymbol{H}_e & \boldsymbol{H}_{em} \\ \boldsymbol{H}_{em}^T & \boldsymbol{H}_m \end{bmatrix} \in R^{(6+n)\times(6+n)}$ *are symmetric and uniformly positive-definite for all* $\boldsymbol{x}_e \in R^{6\times 1}$, $\boldsymbol{\phi} \in R^{n\times 1}$.

n	:	number of the joints.
$\boldsymbol{v}_e$	$\in R^{3\times 1}$:	linear velocity of the end-effector.
$\boldsymbol{\omega}_e$	$\in R^{3\times 1}$:	angular velocity of the end-effector.
$\dot{\boldsymbol{x}}_e = \left[\boldsymbol{v}_e^T \boldsymbol{\omega}_e^T\right]^T$	$\in R^{6\times 1}$:	spatial velocity of the end-effector.
$\boldsymbol{\phi}$	$\in R^{n\times 1}$:	vector for the joint angle of the arm.
$\boldsymbol{H}_e(\boldsymbol{x}_e, \boldsymbol{\phi})$	$\in R^{6\times 6}$:	inertia matrix of the end-effector.
$\boldsymbol{H}_m(\boldsymbol{x}_e, \boldsymbol{\phi})$	$\in R^{n\times n}$:	inertia matrix of the robot arm.
$\boldsymbol{H}_{em}(\boldsymbol{x}_e, \boldsymbol{\phi})$	$\in R^{6\times n}$:	coupling inertia matrix between the end-effector and the arm.
$\boldsymbol{c}_e(\boldsymbol{x}_e, \dot{\boldsymbol{x}}_e, \boldsymbol{\phi}, \dot{\boldsymbol{\phi}})$	$\in R^{6\times 6}$:	non-linear velocity dependent term on the end-effector.
$\boldsymbol{c}_m(\boldsymbol{x}_e, \dot{\boldsymbol{x}}_e, \boldsymbol{\phi}, \dot{\boldsymbol{\phi}})$	$\in R^{n\times n}$:	non-linear velocity dependent term of the arm.
$\boldsymbol{c}_{em}(\boldsymbol{x}_e, \dot{\boldsymbol{x}}_e, \boldsymbol{\phi}, \dot{\boldsymbol{\phi}})$	$\in R^{6\times n}$:	coupling non-linear velocity dependent term between the end-effector and the arm.
$\mathcal{F}_e$	$\in R^{6\times 1}$:	force and moment exerted on the end-effector.
$\mathcal{F}_b$	$\in R^{6\times 1}$:	force and moment exerted on the base.
$\mathcal{F}_i = -\boldsymbol{H}_{em}\ddot{\boldsymbol{\phi}} - \boldsymbol{c}_{em}\dot{\boldsymbol{\phi}}$	$\in R^{6\times 1}$:	reaction force and moment due to the motion of the robot arm.
$\boldsymbol{\tau}$	$\in R^{n\times 1}$:	torque on the joints.
$\mathcal{L}_e$	$\in R^{6\times 1}$:	total linear and angular momentum around the end-effector.
$\boldsymbol{J}_e$	$\in R^{6\times 6}$:	Jacobian matrix related to the end-effector and the base.
$\boldsymbol{J}_m$	$\in R^{6\times n}$:	Jacobian matrix related to the arm and the base.

Table 1. Main notations in dynamic equations

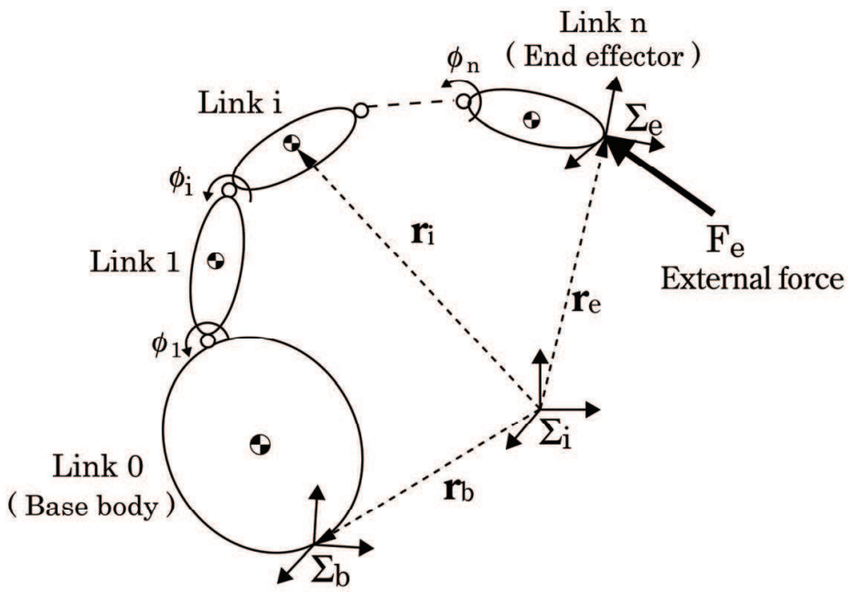

Figure 2. General model for a space robot

Property 2: The following matrices are skew-symmetric :

$$\boldsymbol{S}_e = \boldsymbol{c}_e - \frac{1}{2}\dot{\boldsymbol{H}}_e, \;\; \boldsymbol{S}_m = \boldsymbol{c}_m - \frac{1}{2}\dot{\boldsymbol{H}}_m, \;\; \boldsymbol{S} = \boldsymbol{c} - \frac{1}{2}\dot{\boldsymbol{H}},$$

so that:

$$\boldsymbol{\nu}_e^T \boldsymbol{S}_e \boldsymbol{\nu}_e = 0, \boldsymbol{\nu}_m^T \boldsymbol{S}_m \boldsymbol{\nu}_m = 0, \boldsymbol{\nu}^T \boldsymbol{S} \boldsymbol{\nu} = 0,$$

for all $\boldsymbol{\nu}_e \in R^{6\times 1}$, $\boldsymbol{\nu}_m \in R^{n\times 1}$ *and* $\boldsymbol{\nu} \in R^{(6+n)\times 1}$, *respectively.* $\boldsymbol{c} = \begin{bmatrix} \boldsymbol{c}_e & \boldsymbol{c}_{em} \\ \boldsymbol{c}_{em}^T & \boldsymbol{c}_m \end{bmatrix} \in R^{(6+n)\times(6+n)}$.

2.2 Equations of motion in operational space

The upper part of (1) clearly describes the equation of motion in operational space:

$$\boldsymbol{H}_e \ddot{\boldsymbol{x}}_e + \boldsymbol{H}_{em}\ddot{\boldsymbol{\phi}} + \boldsymbol{c}_e \dot{\boldsymbol{x}}_e + \boldsymbol{c}_{em}\dot{\boldsymbol{\phi}} = \mathcal{F}_e + \boldsymbol{J}_e^T \mathcal{F}_b. \tag{2}$$

In the free-floating space robot, only the joint motion can be considered as the generalized coordinate.

$$\begin{aligned} \boldsymbol{H}_e \ddot{\boldsymbol{x}}_e + \boldsymbol{c}_e \dot{\boldsymbol{x}}_e &= -\boldsymbol{H}_{em}\ddot{\boldsymbol{\phi}} - \boldsymbol{c}_{em}\dot{\boldsymbol{\phi}} + \mathcal{F}_e + \boldsymbol{J}_e^T \mathcal{F}_b \\ &= \mathcal{F}_i + \mathcal{F}_e + \boldsymbol{J}_e^T \mathcal{F}_b \;, \end{aligned} \tag{3}$$

where $\mathcal{F}_i = -\boldsymbol{H}_{em}\ddot{\boldsymbol{\phi}} - \boldsymbol{c}_{em}\dot{\boldsymbol{\phi}} \in R^{6\times 1}$ stands for a reaction force onto the end-effector due to the robot arm motion.

Remark 1: Input command for the operational space dynamics

The right-hand side in (3) apparently shows the reaction or coupling effect due to the motion of the robot arm with joint acceleration expression. The torque control input does not appear explicitly in (3). Joint acceleration, however, can be achieved by velocity-based

closed-loop servo controller straightforwardly as noted in [Konno et al., 1997]. Therefore, eq. (3) are convenient formulation for constructing a control strategy. Hereafter, $\ddot{\boldsymbol{\phi}}$ is considered as an input command to the system and the appropriate joint acceleration for proper control law is computed. Then, one can refer $\mathcal{F}_i = -\boldsymbol{H}_{em}\ddot{\boldsymbol{\phi}} - \boldsymbol{c}_{em}\dot{\boldsymbol{\phi}}$ as a reaction force due to the motion of the robot arm, which can be used to analyze the influence of the parameter errors in Section 4.

Remark 2: Linearity in the Dynamic Parameters

The linearity of eq. (2) is one of the significant features in the articulated-body system. This characteristic plays a key role in the derivation of an adaptive control. The integral of eq. (2) represents the total linear and angular momentum around the center of mass of the end-effector. Then, on the assumption that no active force and torque are applied on the base (e.g. $\mathcal{F}_b$ = 0), eq. (2) can be described as the time-derivative of the momentum $\mathcal{L}_e \in R^{6\times 1}$ as follows:

$$\mathcal{F}_e = \frac{d}{dt}\mathcal{L}_e = \boldsymbol{H}_e\ddot{\boldsymbol{x}}_e + \boldsymbol{H}_{em}\ddot{\boldsymbol{\phi}} + \boldsymbol{c}_e\dot{\boldsymbol{x}}_e + \boldsymbol{c}_{em}\dot{\boldsymbol{\phi}}, \tag{4}$$

$$\begin{aligned}\mathcal{L}_e &= \boldsymbol{H}_e\dot{\boldsymbol{x}}_e + \boldsymbol{H}_{em}\dot{\boldsymbol{\phi}} \\ &= \sum_{i=0}^{n}\begin{bmatrix} m_i\dot{\boldsymbol{r}}_i \\ \boldsymbol{I}_i\boldsymbol{\omega}_i + (\boldsymbol{r}_i - \boldsymbol{r}_e)\times m_i\dot{\boldsymbol{r}}_i \end{bmatrix},\end{aligned} \tag{5}$$

where $\boldsymbol{I}_i, \boldsymbol{\omega}_i$ and m_i stand for the inertia matrix, angular velocity and mass of the link *i*, respectively, $\boldsymbol{r}_i$ and $\boldsymbol{r}_e$ denote the vector from the inertial frame to the center of mass of the link *i* and that from the inertial frame to the center of mass of the end-effector, respectively (see Fig. 2). Once eq. (5) can be linearized with respect to a suitable set of dynamic parameters, eq. (4) can be linear in terms of the dynamic parameters since the dynamic parameters are independent on the motion of the system.

Through some calculations, eq. (5) is linearized in terms of a set of arbitrary dynamic parameters $\boldsymbol{a}$.

$$\mathcal{L}_e = \boldsymbol{y}(\boldsymbol{x}_e, \dot{\boldsymbol{x}}_e, \boldsymbol{\phi}, \dot{\boldsymbol{\phi}})\boldsymbol{a}. \tag{6}$$

Then eq. (4) can be expressed as a function of $\boldsymbol{a}$.

$$\mathcal{F}_e = \boldsymbol{H}_e\ddot{\boldsymbol{x}}_e + \boldsymbol{H}_{em}\ddot{\boldsymbol{\phi}} + \boldsymbol{c}_e\dot{\boldsymbol{x}}_e + \boldsymbol{c}_{em}\dot{\boldsymbol{\phi}} = \boldsymbol{Y}(\boldsymbol{x}_e, \dot{\boldsymbol{x}}_e, \ddot{\boldsymbol{x}}_e, \boldsymbol{\phi}, \dot{\boldsymbol{\phi}}, \ddot{\boldsymbol{\phi}})\boldsymbol{a}, \tag{7}$$

where $\boldsymbol{Y}$ stands for the time-derivative of $\boldsymbol{y}$, which is a function of state values and is called the *regressor*. The choice of the regressor $\boldsymbol{Y}$ and the dynamic parameter vector $\boldsymbol{a}$ is generally arbitrary. In this chapter, we assume that only a grasped target, attached on the end-effector, includes unknown dynamic parameters. The dynamic parameters of the rest of the system and the kinematic parameters are supposed to be well-identified in advance. Therefore, the unknown dynamic parameter vector $\boldsymbol{a}$ is defined as a *p*-dimensional vector containing the mass, center of mass, moment of inertia and product of inertia of the target. Note that $\boldsymbol{a}$ defined here is *constant*.

$$\boldsymbol{a} = (m, r_{gx}, r_{gy}, r_{gz}, I_{xx}, I_{yy}, I_{zz}, I_{xy}, I_{yz}, I_{zx})^T \quad (p = 10).$$

3. Trajectory Control in Operational Space

This section shows the trajectory controller in operational space for a free-floating space robot. The control law shown in this section is derived based on the passivity theorem [van der Schaf, 2000].

3.1 Passivity based trajectory tracking control

Let us define a reference output velocity $\boldsymbol{\eta}$ and a reference output acceleration $\dot{\boldsymbol{\eta}}$ as follows:

$$\boldsymbol{\eta} = \dot{\boldsymbol{x}}_e^d + \boldsymbol{K}_v \tilde{\boldsymbol{x}}_e,$$
$$\dot{\boldsymbol{\eta}} = \ddot{\boldsymbol{x}}_e^d + \boldsymbol{K}_v \dot{\tilde{\boldsymbol{x}}}_e,$$

where $\boldsymbol{K}_v \in R^{6\times 6}$ is a strictly positive definite matrix. $\dot{\boldsymbol{x}}_e^d = \left(\boldsymbol{v}_e^{dT}, \boldsymbol{\omega}_e^{dT}\right)^T \in R^{6\times 1}$ represents the desired velocity in operational space. $\tilde{\boldsymbol{x}}_e = \left(\boldsymbol{e}_p^T, \boldsymbol{e}_O^T\right)^T \in R^{6\times 1}$ depicts the operational space error consisting of the position error $\boldsymbol{e}_p \in R^{3\times 1}$ and the orientation error $e_o \in R^{3\times 1}$. The position error $\boldsymbol{e}_p$ is expressed as:

$$\boldsymbol{e}_p = \boldsymbol{r}_e^d - \boldsymbol{r}_e.$$

The orientation error $\boldsymbol{e}_o$ is expressed by means of the quaternion expression $\mathcal{Q} = \left[\xi, \boldsymbol{\epsilon}^T\right]$ where ξ and $\boldsymbol{\epsilon}$ are the scalar and vector part of the quaternion:

$$\boldsymbol{e}_o = \Delta\boldsymbol{\epsilon} = \xi\boldsymbol{\epsilon}^d - \xi^d\boldsymbol{\epsilon} - \boldsymbol{\epsilon}^d \times \boldsymbol{\epsilon}\ ,$$

where the operator $\times$ denotes the cross-product operator.
The reference error $\boldsymbol{s}$ between the reference output $\boldsymbol{\eta}$ and the actual velocity $\dot{\boldsymbol{x}}_e$ can be described by:

$$\boldsymbol{s} = \boldsymbol{\eta} - \dot{\boldsymbol{x}}_e = \dot{\tilde{\boldsymbol{x}}}_e + \boldsymbol{K}_v \tilde{\boldsymbol{x}}_e. \tag{8}$$

In the case without any parameter errors, the trajectory tracking control law can be determined by using the feedback linearization as follows:

$$\ddot{\boldsymbol{\phi}}^u = -\boldsymbol{H}_{em}^{+}(\boldsymbol{H}_e\dot{\boldsymbol{\eta}} + \boldsymbol{c}_e\boldsymbol{\eta} + \boldsymbol{c}_{em}\dot{\boldsymbol{\phi}} + \boldsymbol{\Lambda}\boldsymbol{s}), \tag{9}$$

where $\boldsymbol{\Lambda} \in R^{6\times 6}$ denotes a positive definite symmetric constant matrix. $\{\cdot\}^u$ stands for the input command and $\{\cdot\}^+$ denotes the pseudo-inverse operator. Note that the control law (9) can be achieved under the condition when $\boldsymbol{H}_{em}$ is nonsingular. Since several researches have already been proposed the treatment of the singularity problem [Nenchev et al., 2000,Tsumaki et al., 2001, Senft & Hirzinger, 1995, Nakamura & Hanafusa, 1986], it is out of focus in this chapter.

3.2 Stability analysis

The stability of the control law (9) can be analyzed by means of the Lyapunov direct method. The following reference error energy is considered as a Lyapunov function:

$$E(t) = \frac{1}{2}\boldsymbol{s}^T \boldsymbol{H}_e \boldsymbol{s}. \tag{10}$$

The time-derivative of E is given as:

$$\begin{aligned}\dot{E}(t) &= \boldsymbol{s}^T(\boldsymbol{H}_e\dot{\boldsymbol{s}} + \frac{1}{2}\dot{\boldsymbol{H}}_e\boldsymbol{s}) \\ &= \boldsymbol{s}^T(\boldsymbol{H}_e\dot{\boldsymbol{\eta}} - \boldsymbol{H}_e\ddot{\boldsymbol{x}}_e + \frac{1}{2}\dot{\boldsymbol{H}}_e\boldsymbol{s}) \\ &= \boldsymbol{s}^T(\boldsymbol{H}_e\dot{\boldsymbol{\eta}} + \boldsymbol{H}_{em}\ddot{\boldsymbol{\phi}} + \boldsymbol{c}_e\boldsymbol{\eta} + \boldsymbol{c}_{em}\dot{\boldsymbol{\phi}}) ,\end{aligned} \tag{11}$$

where *Property 2* in Section 2 is used. Since the control command is expressed in eq. (9), ($\ddot{\boldsymbol{\phi}} = \ddot{\boldsymbol{\phi}}^u$ noted in *Remark 1* in Section 2), the time-derivative of $E(t)$ results in:

$$\dot{E}(t) = -\boldsymbol{s}^T\boldsymbol{\Lambda}\boldsymbol{s} \leq 0. \tag{12}$$

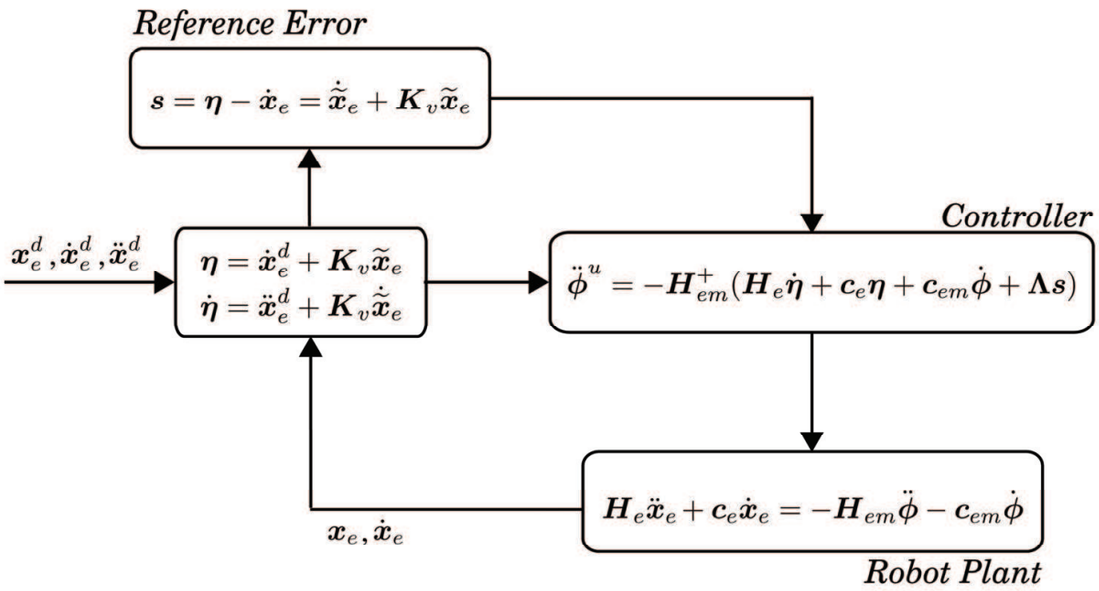

Figure 3. Control diagram for trajectory tracking

Consequently, the result of $\dot{E}$ holds always semi-negative and the closed-loop system (2) with (9) is guaranteed to be asymptotically stable. The inequality (12) implies that the steady-state reference error $\boldsymbol{s}$ converges asymptotically to zero, which leads to the convergence of the steady-state position. The control diagram for operational tracking control is shown in Fig. 3.

4. Adaptive Control

The previous section explained the trajectory control for a free-floating space robot based on the inverted chain approach on the assumption of no dynamic parameter errors. In practical situations, however, the robot arm handles various components whose dynamic properties

are not known in advance. Those model inaccuracies may lead to the degradation of the control performance and the deviation of the trajectory tracking from the desired one.
This section proposes an adaptive control for a free-floating space robot against the parameter uncertainties.

4.1 Influence of the dynamic parameter errors

In the presence of dynamic parameter inaccuracies, the dynamic model in operational space can be described as follows:

$$\widehat{\boldsymbol{H}}_e\ddot{\boldsymbol{x}}_e + \widehat{\boldsymbol{c}}_e\dot{\boldsymbol{x}}_e = -\widehat{\boldsymbol{H}}_{em}\ddot{\boldsymbol{\phi}} - \widehat{\boldsymbol{c}}_{em}\dot{\boldsymbol{\phi}} = \widehat{\mathcal{F}}_i, \tag{13}$$

where $\widehat{\{\cdot\}}$ stands for the matrix including dynamic parameter errors. In analogy with (9), the control law derived from the dynamic model (13) becomes:

$$\ddot{\boldsymbol{\phi}}^u = -\widehat{\boldsymbol{H}}_{em}^{+}(\widehat{\boldsymbol{H}}_e\dot{\boldsymbol{\eta}} + \widehat{\boldsymbol{c}}_e\boldsymbol{\eta} + \widehat{\boldsymbol{c}}_{em}\dot{\boldsymbol{\phi}} + \boldsymbol{\Lambda}\boldsymbol{s}). \tag{14}$$

In the implementation of the input command (14) to the dynamic system (2), the reaction force due to the motion of the robot arm $\mathcal{F}_i$ and the corresponding expected reaction force $\widehat{\mathcal{F}}_i$ has error $\widetilde{\mathcal{F}}_i$.

$$\begin{aligned}\widetilde{\mathcal{F}}_i &= \mathcal{F}_i - \widehat{\mathcal{F}}_i \\ &= -\boldsymbol{H}_{em}\ddot{\boldsymbol{\phi}}^u + \widehat{\boldsymbol{H}}_{em}\ddot{\boldsymbol{\phi}}^u - \boldsymbol{c}_{em}\dot{\boldsymbol{\phi}} + \widehat{\boldsymbol{c}}_{em}\dot{\boldsymbol{\phi}} \\ &= -\widetilde{\boldsymbol{H}}_{em}\ddot{\boldsymbol{\phi}}^u - \widetilde{\boldsymbol{c}}_{em}\dot{\boldsymbol{\phi}},\end{aligned} \tag{15}$$

where $\widetilde{\{\cdot\}}$ stands for the error matrix. With the input acceleration (14), the reaction force $\mathcal{F}_i$ can be described by the corresponding expected force $\widehat{\mathcal{F}}_i$ and the error $\widetilde{\mathcal{F}}_i$ as follows:

$$\begin{aligned}\mathcal{F}_i &= \widehat{\mathcal{F}}_i + \widetilde{\mathcal{F}}_i \\ &= \widehat{\boldsymbol{H}}_e\dot{\boldsymbol{\eta}} + \widehat{\boldsymbol{c}}_e\boldsymbol{\eta} + \boldsymbol{\Lambda}\boldsymbol{s} - \widetilde{\boldsymbol{H}}_{em}\ddot{\boldsymbol{\phi}}^u - \widetilde{\boldsymbol{c}}_{em}\dot{\boldsymbol{\phi}}.\end{aligned} \tag{16}$$

Let us analyze here the stability of the system containing the dynamic parameter errors by using the Lyapunov function (10). In the closed-loop system (2) with the controller (14), the time-derivative of the Lyapunov function (10) is given by:

$$\begin{aligned}\dot{E}(t) &= \boldsymbol{s}^T(\boldsymbol{H}_e\dot{\boldsymbol{\eta}} + \boldsymbol{H}_{em}\ddot{\boldsymbol{\phi}} + \boldsymbol{c}_e\boldsymbol{\eta} + \boldsymbol{c}_{em}\dot{\boldsymbol{\phi}}) \\ &= \boldsymbol{s}^T(\widetilde{\boldsymbol{H}}_e\dot{\boldsymbol{\eta}} + \widetilde{\boldsymbol{H}}_{em}\ddot{\boldsymbol{\phi}}^u + \widetilde{\boldsymbol{c}}_e\boldsymbol{\eta} + \widetilde{\boldsymbol{c}}_{em}\dot{\boldsymbol{\phi}} - \boldsymbol{\Lambda}\boldsymbol{s})\ ,\end{aligned} \tag{17}$$

where *Remark 1* is used, namely $\ddot{\boldsymbol{\phi}} = \ddot{\boldsymbol{\phi}}^u$.As mentioned in *Remark* 2, the dynamic system is linearized with the vector of dynamic parameters $\boldsymbol{a}$ and the regressor $\boldsymbol{Y}$. Then, the above time-derivative can be rewritten as:

$$\dot{E}(t) = \boldsymbol{s}^T(\ \boldsymbol{Y}\widetilde{\boldsymbol{a}} - \boldsymbol{\Lambda}\boldsymbol{s}\ ), \tag{18}$$

where $\widetilde{\boldsymbol{a}} = \boldsymbol{a} - \widehat{\boldsymbol{a}}$ denotes the parameter estimation error vector, $\boldsymbol{a}$ is a p-dimensional vector including the unknown dynamic parameters and $\widehat{\boldsymbol{a}}$ is its estimate. The above equality indicates that each component Λ_i in the gain matrix $\boldsymbol{\Lambda}$ needs to meet the following condition in order to obtain the robust system against the model inaccuracies:

$$\Lambda_i \geq [\boldsymbol{Y}\widetilde{\boldsymbol{a}}]_i + \mu_i \ , \ \left(i = 1 \cdots 6 \right) , \tag{19}$$

where the constant μ_i is strictly positive. As long as the above condition holds, the controller (14) is robust against the parameter inaccuracies and the tracking error converges to zero.

4.2 Adaptive controller design

Equation (17) suggests two solutions to compensate the parameter uncertainty in the system. One is the improvement of the robustness in the control law (14) with proper design of the gain matrix as shown in (19). The other is to adjust the dynamic parameter itself during the operation, which is called an *adaptive control* [Slotine & Li, 1987] [Slotine & Li, 1988].

This section proposes an adaptive control in the case without any knowledge of the dynamic parameters in advance, such that the space robot grasps a target whose dynamic parameters are unknown.

Let us consider the following Lyapunov function described with the sum of the reference error energy of the system (10) and the potential energy due to the model uncertainties:

$$V(t) = E(t) + \frac{1}{2}\widetilde{\boldsymbol{a}}^T \boldsymbol{\Gamma} \widetilde{\boldsymbol{a}}, \tag{20}$$

where $\boldsymbol{\Gamma} \in R^{p \times p}$ is a positive definite matrix. The time-derivative of (20) becomes:

$$\dot{V}(t) = -\boldsymbol{s}^T \boldsymbol{\Lambda} \boldsymbol{s} + \widetilde{\boldsymbol{a}}^T (\boldsymbol{Y}^T \boldsymbol{s} + \boldsymbol{\Gamma} \dot{\widetilde{\boldsymbol{a}}}). \tag{21}$$

This suggests the following condition should be met to guarantee the system stability,

$$\boldsymbol{Y}^T \boldsymbol{s} + \boldsymbol{\Gamma} \dot{\widetilde{\boldsymbol{a}}} = 0. \tag{22}$$

Then, the following adaptive control law is derived as:

$$\dot{\widetilde{\boldsymbol{a}}} = -\boldsymbol{\Gamma}^{-1} \boldsymbol{Y}^T \boldsymbol{s}, \tag{23}$$

where $\widetilde{\boldsymbol{a}} = \boldsymbol{a} - \widehat{\boldsymbol{a}}$ and the parameter vector $\boldsymbol{a}$ is constant.

Consequently, the time-derivative of the Lyapunov function results in:

$$\dot{V}(t) = -\boldsymbol{s}^T \boldsymbol{\Lambda} \boldsymbol{s} \leq 0. \tag{24}$$

The inequality (24) indicates the reference error $\boldsymbol{s}$ converges asymptotically to zero if and only if $\dot{\widetilde{\boldsymbol{x}}}_e \to \boldsymbol{0}$ and $\widetilde{\boldsymbol{x}}_e \to \boldsymbol{0}$. Accordingly, the control law for the trajectory tracking in operational space (14) and the adaptation law (23) yield a stable adaptive controller. Fig. 4 shows the control diagram for the proposed adaptive control.

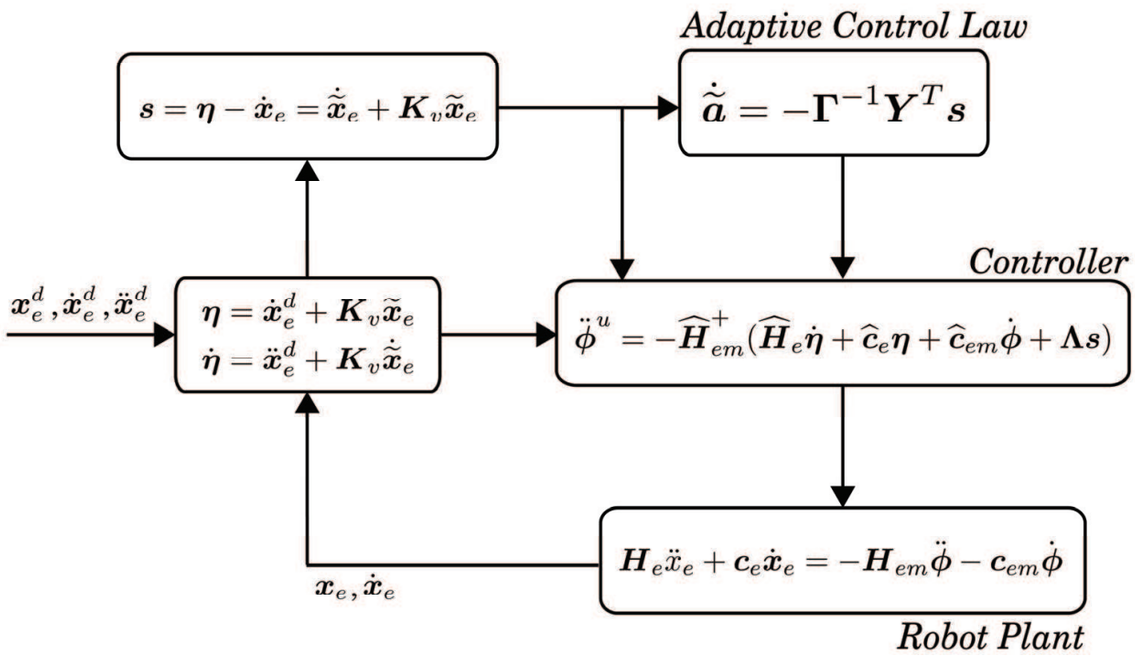

Figure 4. Control diagram for an adaptive trajectory tracking control in operational space

5. Composite Adaptive Control

The adaptive controller developed in the previous section exploits the tracking error to extract the parameter information. To obtain the parameter information, however, one can find various candidates [Slotine & Li, 1991]. One possible candidate is the prediction error, which is generally used for parameter estimation. In this section, an alternative adaptive control law is developed with the combination of the tracking error and the reaction force error. The reaction forces due to the motion of the robot-arm are assumed to be measured by the force/torque sensor attached on the end-effector, to which the target is attached. The measurement values are used for parameter adaptation together with the nominal adaptive control law (23).

5.1 Composite adaptive controller design

In analogy with Section 2, the reaction forces on the end-effector are able to be linearized with a proper set of the dynamic parameters $\boldsymbol{a}$ as $\mathcal{F}_e^{F/T} = \boldsymbol{W}\boldsymbol{a}$ and its prediction error can be described as $\tilde{\mathcal{F}}_e^{F/T} = \boldsymbol{W}\tilde{\boldsymbol{a}}$, where $\boldsymbol{W}$ stands for the regressor. The detail derivation is omitted in this chapter.

The adaptive control law (23) is extended to the following expression combined with the tracking error and the predicted reaction force error:

$$\dot{\tilde{\boldsymbol{a}}} = -\boldsymbol{\Gamma}^{-1}\{\boldsymbol{Y}^T\boldsymbol{s} + \boldsymbol{W}^T\boldsymbol{R}\tilde{\mathcal{F}}_e^{F/T}\}\,, \tag{25}$$

where $\boldsymbol{R} \in R^{6\times 6}$ is a uniformly weighting matrix. Eq. (25) can be rewritten as:

$$\dot{\tilde{\boldsymbol{a}}} + \boldsymbol{\Gamma}^{-1}\boldsymbol{W}^T\boldsymbol{R}\boldsymbol{W}\tilde{\boldsymbol{a}} = -\boldsymbol{\Gamma}^{-1}\boldsymbol{Y}^T\boldsymbol{s}, \tag{26}$$

which indicates a time-varying low-pass filter and that parameter and tracking error convergence in composite adaptive control can be smoother and faster than in the nominal adaptive control only.

To analyze the stability of the system applied the above composite adaptive control law and the trajectory tracking control, the Lyapunov function (20) is considered again. The time-derivative of (20) is derived as (21). Since the adaptive control law is determined by (25), substitution of (25) into (21) leads to the following inequality:

$$\dot{V}(t) = -\boldsymbol{s}^T\boldsymbol{\Lambda}\boldsymbol{s} - \tilde{\boldsymbol{a}}^T\boldsymbol{W}^T\boldsymbol{R}\boldsymbol{W}\tilde{\boldsymbol{a}} \leq 0, \tag{27}$$

which describes that the reference error $\boldsymbol{s}$ and the prediction error $\tilde{\mathcal{F}}_e^{F/T}$ globally converge to zero if the desired trajectories are bounded. If the trajectories are persistently exciting and uniformly continuous, the estimated parameters converge asymptotically to the real ones. Fig. 5 shows the control diagram for the proposed composite adaptive control.

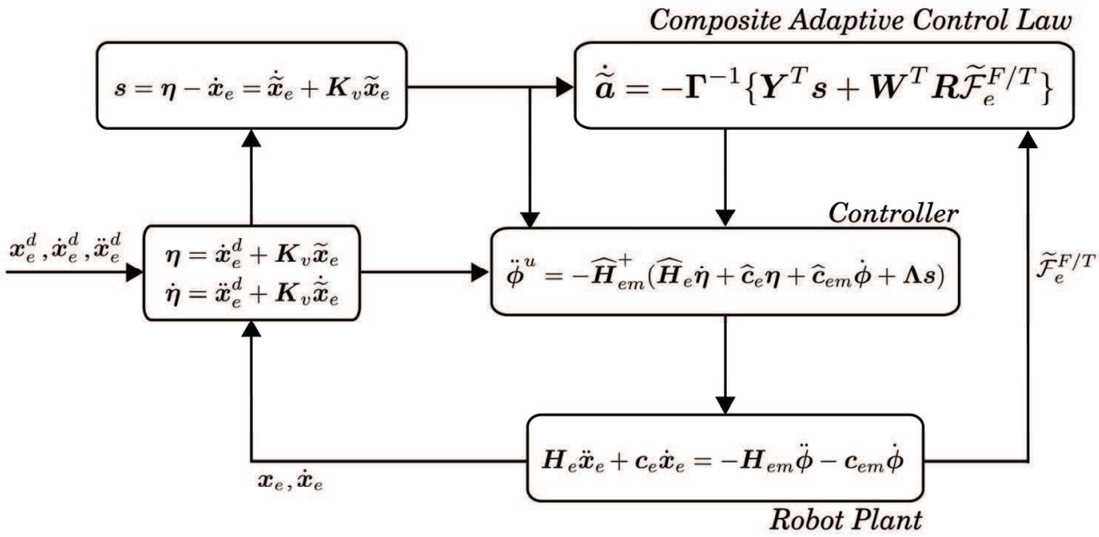

Figure 5. Control diagram for a composite adaptive trajectory tracking control in operational space

6. Simulation Study

This section presents the numerical simulation results of a realistic three-dimensional model as shown in Fig. 1. In this simulation, the chaser-robot is assumed to track a given trajectory while it grasps firmly a target including unknown dynamic properties. The dynamic parameters of the rest of the system and the kinematic parameters are supposed to be well-identified in advance. The initial total linear and angular momentum for whole system are zero in the simulation. During the tracking phase, no external force is applied. The chaser robot has a 7DOF manipulator mounted on the base satellite, whose dynamic parameters are shown in Table 2. The robot arm has one redundancy with respect to the

end-effector motion, then the null-space can be used for an additional task. In the simulation examples, the target parameters of the planned motion are supposed to be zero, while those of the controlled motion are in Table 3, giving the extent of uncertainty introduced in the system. As mentioned in Section 2, the vector of the unknown dynamic parameters $\boldsymbol{a}$ is defined as follows:

$$\boldsymbol{a} = (m, r_{gx}, r_{gy}, r_{gz}, I_{xx}, I_{yy}, I_{zz}, I_{xy}, I_{yz}, I_{zx})^T \quad (p = 10).$$

The adaptation gain $\boldsymbol{\Gamma}^{-1}$ in eq. (23) is determined as:

$$\boldsymbol{\Gamma}^{-1} = diag([\, 5 \times 10^3,\ 10,\ 10,\ 10,\ 5 \times 10^2,\ 5 \times 10^2,\ 5 \times 10^2,\ 5 \times 10^{-4},\ 5 \times 10^{-4},\ 5 \times 10^{-4}\,]).$$

The control gains $\boldsymbol{\Lambda}$ and $\boldsymbol{K}_v$ in eq. (14) are set to be:

$$\boldsymbol{\Lambda} = diag([\, 20,\ 20,\ 20,\ 3000,\ 3000,\ 3000\,]),$$
$$\boldsymbol{K}_v = diag([\, 10,\ 10,\ 10,\ 1000,\ 1000,\ 1000\,]).$$

The weighing matrix $\boldsymbol{R}$ in the composite adaptive control (25) is determined as:

$$\boldsymbol{R} = diag([\, 0.5,\ 0.5,\ 0.5,\ 0.5,\ 0.5,\ 0.5\,]).$$

	mass [*kg*]	I_{xx} [kgm^2]	I_{yy} [kgm^2]	I_{zz} [kgm^2]
Base	140	18.0	20.0	22.0

	mass [*kg*]	I_{xx} [kgm^2]	I_{yy} [kgm^2]	*Izz* [kgm^2]
Each Link	3.3	0.0056	0.0056	0.0056

Table 2. Dynamic parameters for a chaser-robot

mass [*kg*]	I_{xx} [kgm^2]	I_{yy} [kgm^2]	I_{zz} [kgm^2]
87.5	11.25	12.5	12.5

Table 3. Dynamic parameters for a target

	w/oAC	with AC	with CAC
RMS error	0.0141	0.0048	0.0032

Table 4. Root Mean Square error for tracking error

Figs. 6 and 7 illustrate the desired and actual trajectories in Cartesian space. Fig. 6 shows the case with parameter deviations but without adaptive control. Fig. 7 shows the case

with adaptive control (23). The left graphs depict the trajectory in xy plane and the right graphs show the trajectory in xz plane in Cartesian space. In the graphs, the solid line depicts the desired trajectory and the dashed line depicts the actual trajectory, respectively. It is clearly observed that the end effector follows the trajectory when the adaptive control is activated, even though the parameter deviations exist, while in the case without adaptive control law, the end effector deviates the desired trajectory due to the model errors. Fig. 8 depicts the typical examples for the parameter adaptation process when the adaptive control law is applied. In the figure, the adaptation processes of the mass, moment of inertia of each axis are shown. Note here that the adjusted dynamic parameters do not have to converge to the real ones since the demanded task is to follow a given trajectory. If one would like to identify real values, the persistent excitation of the input command is required.

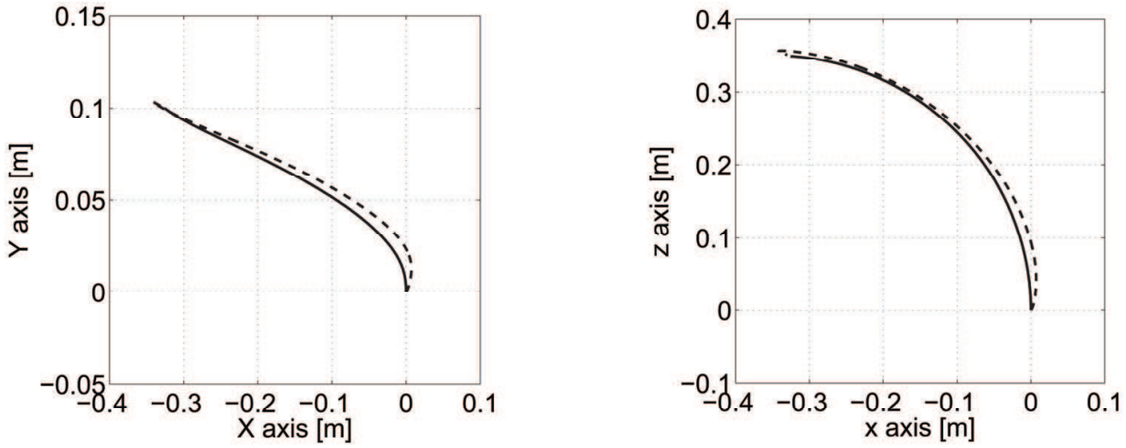

(a) XY Plane (b) XZ Plane

Figure 6. Trajectory without adaptive control

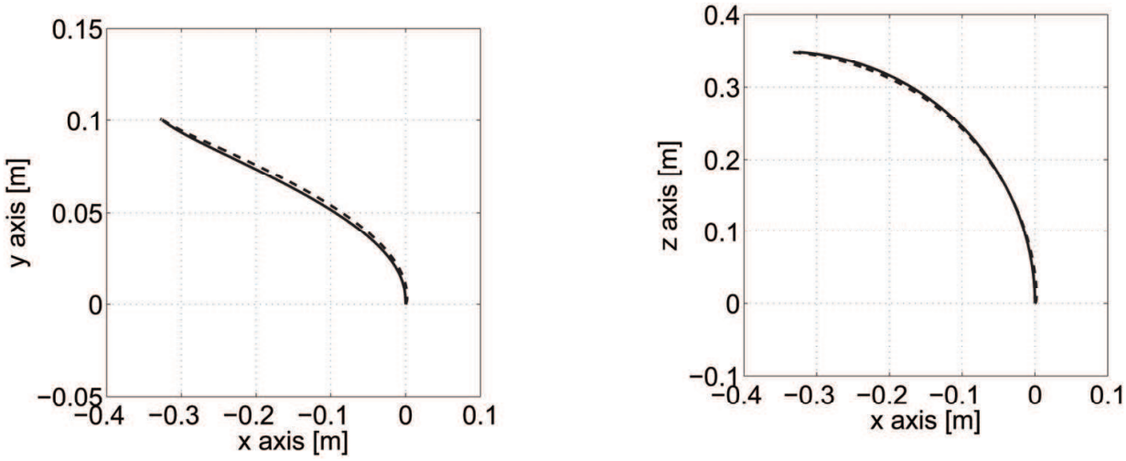

(a) XY Plane (b) XZ Plane

Figure 7. Trajectory with adaptive control

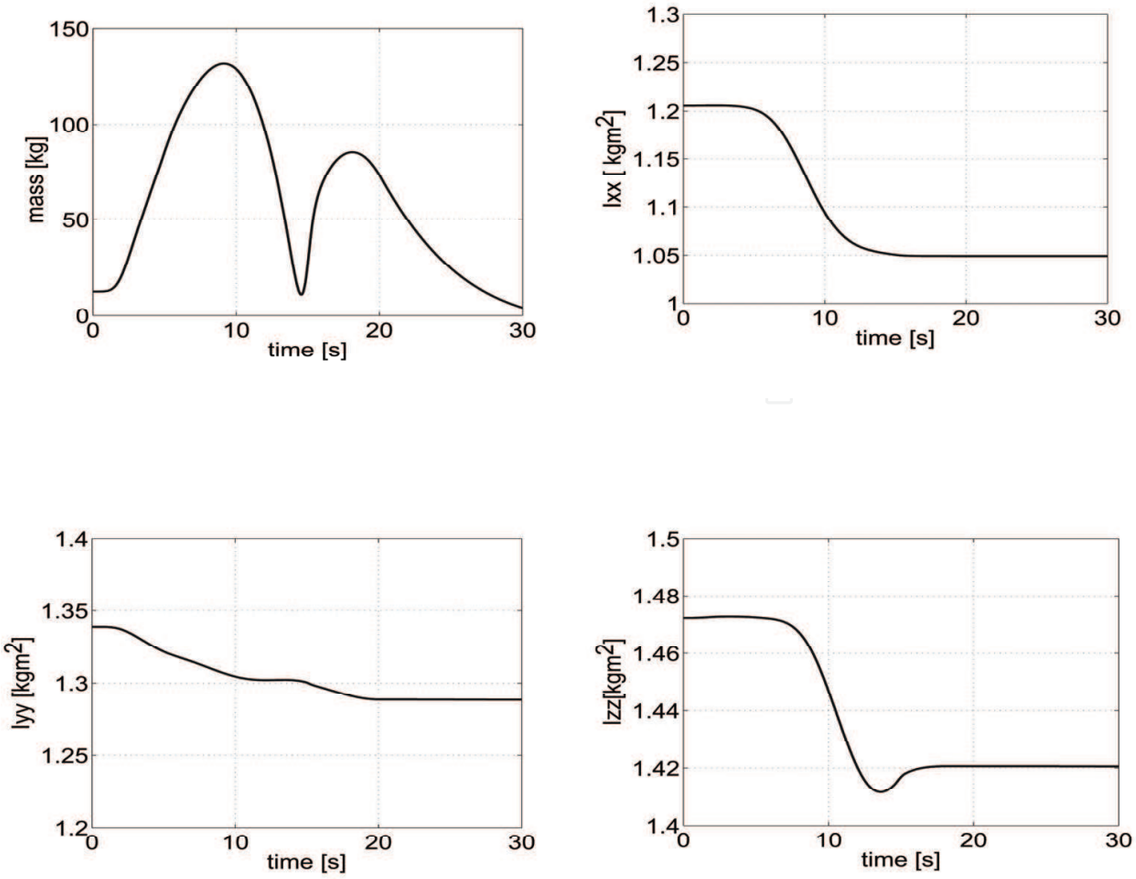

Figure 8. Adaptation process of the parameters

Furthermore, the composite adaptive control (25) is verified in the same condition. The actual trajectory follows the desired one with less tracking error than the normal adaptive control (23) since not only the tracking reference error but also the reaction force error are utilized to extract more information for the unknown dynamic parameters. Table 4 shows the root mean square error(RMSE) of the tracking error for each case. The root mean square error is calculated as follows:

$$RMS\ error = \sqrt{\frac{\sum_{i=1}^{m}\{\boldsymbol{e}_p^T(i)\boldsymbol{e}_p(i)\}}{m}} \tag{28}$$

where m denotes the number of data points in the simulation. The vector $\boldsymbol{e}_p$ depicts the position error of the end-effector described in Section 3. In Table 4, "w/o AC", "with AC" and "with CAC" stand for the case without adaptive control, with adaptive control and the case with composite adaptive control, respectively.

The simulations verify that the proposed adaptive controls are effective to achieve the trajectory tracking against the parameter uncertainties.

7. Conclusions

In this chapter, we proposed an adaptive control for a free-floating space robot by using the inverted chain approach, which is a unique formulation for a space robot compared with that for a ground-based manipulator system. This gives the explicit description of the coupled dynamics between the end-effector and the robot arm, and provides the advantage of linearity with respect to the inertial parameters for the operational space formulation.

In a free-floating space robot, the dynamic parameters affect not only its dynamics but also its kinematics. By paying attention to the internal dynamics between the end-effector motion and the joint motion, we developed an adaptive control for operational space trajectory tracking in the presence of model uncertainties. To improve the adaptive control performance, a composite adaptive control by using the information of the tracking error and the reaction force is further discussed. The proposed control methods are verified by realistic numerical simulations. The simulation results clearly show that the proposed adaptive controls are effective against the dynamic parameter errors.

8. References

Abiko, S.; Lampariello, R. & Hirzinger, G. (2006). Impedance Control for a Free-Floating Robot in the Grasping of a Tumbling Target with Parameter Uncertainty, *Proc. of the 2006 IEEE/RSJ Int. Conf. on Intelligent Robots and Systems,* pp. 1020 - 1025, Beijing, China, Oct. 2006.

Gu, Y. L. & Xu, Y. (1993). A Normal Form Augmentation Approach to Adaptive Control of Space Robot Systems, *Proc. of the 1993 IEEE Int. Conf. on Robotics and Automation,* vol. 2, pp. 731 - 737, Atlanta, USA, May 1993.

Konno, A.; Uchiyama, M.; Kito, Y. & Murakami, M. (1997). Configuration-Dependent Vibration Controllability of Flexible-Link Manipulators, *Int. Journal Robot. Research,* vol. 16, no. 4, pp. 567 - 576, 1997.

Nakamura, Y.; & Hanafusa, H. (1986). Inverse Kinematic Solutions with Singularity Robustness for Robot Manipulator Control, *Journal of Dynamic Systems, Measurement, and Cotnrol*. vol. 108, pp.163 - 171, 1986.

Nenchev, D. N.; Tsumaki, Y. & Uchiyama, M. (2000). Singularity-Consistent Parameterization of Robot Motion and Control, *Int. Journal of Robotics Research,* vol. 19, no. 2, pp. 159 - 182, 2000.

Senft, V. & Hirzinger, G. (1995). Redundant Motions of Non Redundant Robots - A New Approach to Singularity Treatment, *Proc. of the 1995 IEEE Int. Conf. on Robotics and Automation,* pp. 1553 - 1558, Nagoya, Japan, May 1995.

Slotine, J. J. E. & Li, W. (1987). On the Adaptive Control of Robot Manipulators, *The Int. Journal of Robotics Research,* vol. 6, no. 3, pp. 49 - 59, 1987.

Slotine, J. J. E. & Li, W. (1988). Adaptive Manipulator Control: A Case Study, *IEEE Transactions on Automatic Control,* vol. 33, no. 11, pp. 995 - 1003, 1988.

Slotine, J. J. E. & Li, W. (1991). *Applied Nonlinear Control:* Prentice Hall, ISBN 978-0130408907.

Tsumaki, Y; Fiorini, P.; Chalfant, G. & Seraji, H. (2001). A Numerical SC Approach for A Teleoperated 7-DOF Manipulator, *Proc. of the 2001 IEEE Int. Conf. on Robotics and Automation,* pp. 1039 - 1044, Seoul, Korea, May 2001.

van der Schaf, A. (2000). *L_2-Gain and Passivity Techniques in Nonlinear Control:* Spriger-Verlag, ISBN 978-1852330736.

Xu, Y. & Kanade, T. (1993). *Space Robotics: Dynamics and Control:* Kluwer Academic Publishers, ISBN 978-0792392651.

Xu, Y; Shum, H.-Y; Lee, J.-J. & Kanade, T. (1992). Adaptive Control of Space Robot System with an Attitude Controlled Base, *Proc. of the 1992 Int. Conf. on Robotics and Automation,* pp. 2005 - 2011, Nice, France, May 1992.

Frontiers in Adaptive Control

Edited by Shuang Cong

ISBN 978-953-7619-43-5
Hard cover, 334 pages
Publisher InTech
Published online 01, January, 2009
Published in print edition January, 2009

The objective of this book is to provide an up-to-date and state-of-the-art coverage of diverse aspects related to adaptive control theory, methodologies and applications. These include various robust techniques, performance enhancement techniques, techniques with less a-priori knowledge, nonlinear adaptive control techniques and intelligent adaptive techniques. There are several themes in this book which instance both the maturity and the novelty of the general adaptive control. Each chapter is introduced by a brief preamble providing the background and objectives of subject matter. The experiment results are presented in considerable detail in order to facilitate the comprehension of the theoretical development, as well as to increase sensitivity of applications in practical problems

InTech Europe
University Campus STeP Ri
Slavka Krautzeka 83/A
51000 Rijeka, Croatia
Phone: +385 (51) 770 447
Fax: +385 (51) 686 166
www.intechopen.com

InTech China
Unit 405, Office Block, Hotel Equatorial Shanghai
No.65, Yan An Road (West), Shanghai, 200040, China
中国上海市延安西路65号上海国际贵都大饭店办公楼405单元
Phone: +86-21-62489820
Fax: +86-21-62489821

IntechOpen